Star Polymer Catalysts

DOI: 10.1002/anie.201101381

Star-Polymer-Catalyzed Living Radical Polymerization: Microgel-Core Reaction Vessel by Tandem Catalyst Interchange**

Takaya Terashima, Akihisa Nomura, Makoto Ito, Makoto Ouchi, and Mitsuo Sawamoto**

The design and functionalization of reaction space around catalytic centers may promote catalysis.[1–3] With their unique three-dimensional globular structures, microgel-core star polymers[4–8] are intriguing as scaffolds that enclose catalysts: the central core is not only compartmentalized by linear-arm polymers but is also locally heterogeneous (cross-linked network), while the molecule as a whole is completely homogeneous and soluble through its soluble surrounding arms. Given these features, core-functionalized star polymers[5–8] have been developed as a new type of macromolecularly supported catalysts with a unique reaction space. For example, we have synthesized such star polymer catalysts by metal-catalyzed living radical polymerization[9,10] (Scheme 1) by in situ direct encapsulation ("tandem catalyst interchange") of ruthenium complexes into the microgel core that carries multiple phosphine ligands.[5] These "metal-bearing" star polymers efficiently catalyzed hydrogen-transfer reactions with high activity, versatility, and recyclability, in comparison to their homogeneous or polymer-supported counterparts.[3]

Herein, we report living radical polymerization in microgel-core reaction vessels of metal-bearing star polymers obtained by tandem catalyst interchange (Scheme 1). These star catalysts are well soluble, but the metal complexes are caged (i.e., protected) within the microgel network and lead to high activity and stability, functionality tolerance, and catalyst recycling, among others. This work is to demonstrate that the star-catalyzed system enables a novel homogeneous compartmentalized polymerization in a catalyst-embedded core, which is to be clearly distinguished from the polymerizations with conventional polymer-supported insoluble catalysts[11] and those in heterogeneous dispersed or emulsion systems particularly in terms of catalytic activity, functionality tolerance, and recyclability, among other feartures expected.[12]

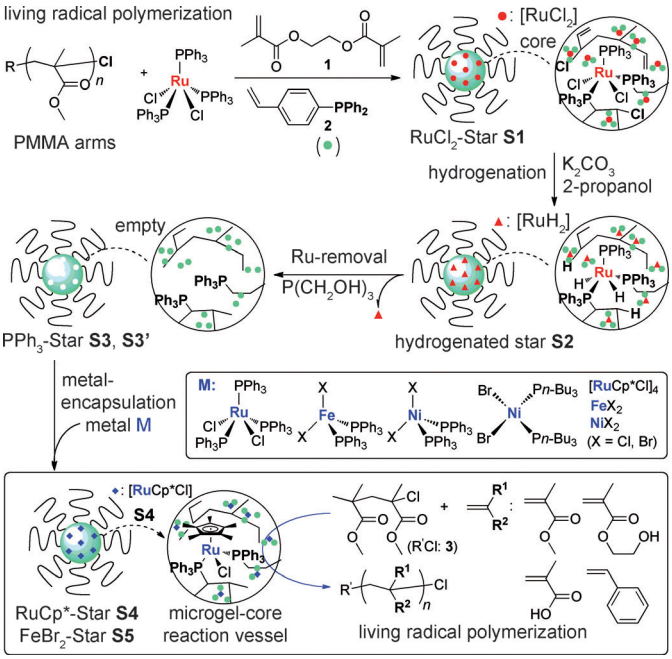

Scheme 1. Synthesis of metal-star catalysts by tandem catalyst interchange and star-polymer-catalyzed living radical polymerization.

To successfully apply star polymer catalysts to the polymerization, PPh_3-star **S3** was synthesized by a one-pot tandem route consisting of: 1) the synthesis of $RuCl_2$-Star **S1** by the ruthenium-catalyzed linking reaction of linear-arm polymers with a binfunctional linker **1** and a ligand comonomer **2**;[5] 2) the in situ hydrogenation[13] of the core-bound chlorine and olefin units within **S1** to give hydrogenated star **S2,** and 3) the removal of the core-bound ruthenium complexes from **S2** leading to an empty-core star **S3** with nonligating phosphines. Then, new metal complexes were introduced into the core of **S3**, giving metal-star catalysts such as RuCp*-Star **S4** to be directly employed for living polymerization. Hence, the original polymerization catalyst $[RuCl_2(PPh_3)_3]$ is first core-bound and then interchanged with a new complex [e.g., RuCp* or $FeBr_2$], all in situ and in one pot. Note that step (2) serves to eliminate the potentially growth-active or reactive units (halogen and olefin, respectively) from the core. The products were characterized by size exclusion chromatography (SEC), multi-angle laser light scattering coupled with SEC (SEC-MALLS), proton and phosphine nuclear magnetic resonance (^{1}H NMR and ^{31}P NMR), UV/Vis, and inductively coupled plasma atomic emission spectroscopy (ICP-AES).

[*] T. Terashima, A. Nomura, M. Ito, M. Ouchi, Prof. M. Sawamoto
Department of Polymer Chemistry, Graduate School of Engineering, Kyoto University
Kyotodaigaku-Katsura, Nishikyo-ku, Kyoto 615-8510 (Japan)
E-mail: terashima@living.polym.kyoto-u.ac.jp
sawamoto@star.polym.kyoto-u.ac.jp

[**] This research was supported by the Ministry of Education, Science, Sports and Culture through a Grant-in Aid for Creative Scientific Research (18GS0209), and through Grant-in Aids for Young Scientist (Start-up) (No.19850010) and Young Scientist (B) (No.20750091), for which T.T. is grateful. We thank Hokko Chemical for the kind supply of diphenylphosphinostyrene (**2**). We acknowledge Dr. Takeshi Niitani and his colleagues (Nippon Soda Co., Ltd.) for ICP-AES analysis.

Supporting information for this article is available on the WWW under http://dx.doi.org/10.1002/anie.201101381.

$RuCl_2$-Star **S1** was directly prepared by the [$RuCl_2$-(PPh_3)$_3$]-mediated living radical polymerization of methyl methacrylate (MMA) with ethyl α-chlorophenylacetate (initiator), followed by the linking reaction of the PMMA arms with **1** and **2** (conversions of MMA, **1**, and **2**: 98%, 93%, and 100%, respectively; star yield: 78%. SEC-MALLS: $M_{w,star}$ = 651,000; number of arms per star, f = 35; R_g = 9.7 nm. ICP-AES: 7500 ppm of Ru; Figure S1, S2, Tables S1, S2: see the Supporting information). The degree of polymerization for the arm (DP = [MMA]$_0$/[initiator]$_0$) was set to 100, and the molar feed ratios of **1** (r_1) and **2** (r_2) to the initiator were 10 and 5.0, respectively. **S1** was sequentially treated with PPh_3 and K_2CO_3 in 2-propanol at 80 °C for hydrogenation.[13] The initially red-brown solution immediately turned yellow, indicating that the **S1**-bound $RuCl_2$ was transformed into the dihydride RuH_2, to give a core-hydrogenated star **S2** (Figure S1). A pure PPh_3-Star (**S3**: white powder) was obtained from the removal of ruthenium from **S2** by the ligand exchange reaction with $P(CH_2OH)_3$[14] (SEC-MALLS: $M_{w,star}$ = 698000, f = 38 arms, R_g = 9.8 nm; ICP-AES: 650 ppm of Ru; Figure 1a, Tables S1, S2). Similarly, nonhydrogenated PPh_3-Star **S3′** was prepared by removal of Ru alone.

S3 exhibited no UV/Vis absorption of ruthenium complexes around 400 to 800 nm (Figure 1b). ICP-AES analysis showed that over 91% ruthenium was removed from **S1** (from 7500 to 650 ppm). **S3** maintained the original shape, overall molecular weight, and size without any collapse of the core during the one-pot core treatment (Figure S1, Table S1). The core-bound phosphines in **S3** were clearly observed as broad signals around δ = 7.3 ppm by ^{1}H NMR spectroscopy and δ = −1 ppm by ^{31}P NMR spectroscopy (Figure 1c and d), in spite of the small peaks in **S1** and **S2** (Figure S1). The number (N_2) of the core-incorporated ligands per **S3** was 182 (by ^{1}H NMR), which is in good agreement with the value calculated from the arm number (f) and the **2**/initiator feed ratio (r_2) ($N_{2,calcd} = fr_2$ = 192). Thus, the core of **S3** carries a large number of "empty" nanocavities surrounded by multiple triphenylphosphine ligands by which $RuCl_2$ was originally trapped.

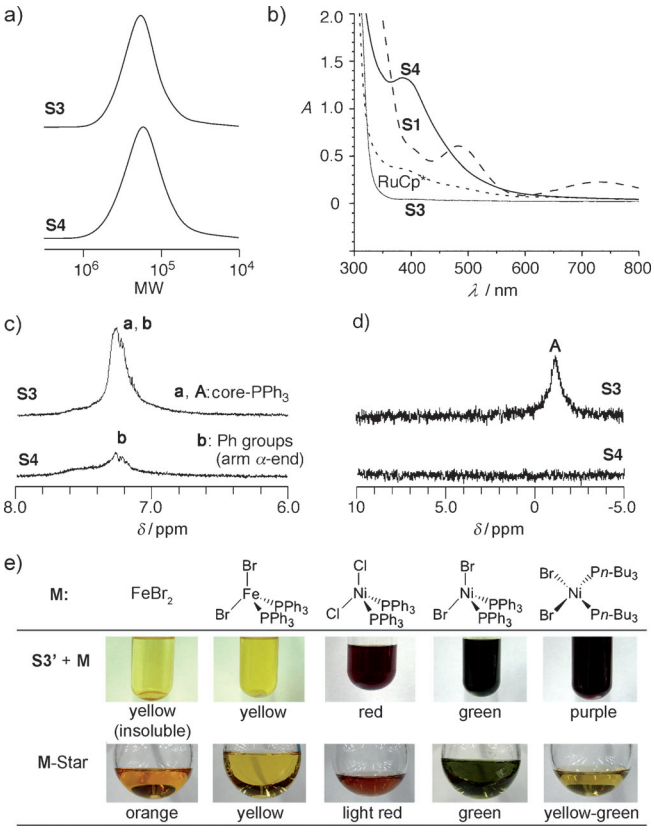

Figure 1. Synthesis of metal-bearing star polymers with **S3** or **S3′**: a) SEC curves of **S3** and **S4** in DMF; b) UV/Vis spectra of **S1**, **S3**, **S4**, and [RuCp*Cl(PPh_3)$_2$] (RuCp*) in dichloroethane at RT, [**S1**, **S3**, **S4**] = 0.0125 g mL^{-1}, [RuCp*] = 0.5 mM; c) ^{1}H NMR spectrum (CD_2Cl_2) and d) ^{31}P NMR spectrum ([D_8]toluene) of **S3** and **S4** at RT; e) photographs of metal-star polymers in toluene.

Introduction of metals (**M**) into these cavities was first examined with the nonhydeogenated star **S3′** by mixing the two components in toluene at 80 °C for 25 h ([PPh_3 in **S3′**]/[**M**] 1:1; Figure 1e, S3, and S4, Table S3). [$RuCl_2(PPh_3)_3$], [MX_2-(PPh_3)$_2$], and [$NiBr_2(PnBu)_2$] as well as their nonligated forms MX_2 (M = Fe, Ni, X = Cl, Br) were efficiently enclosed into the core by ligand exchange. Except for that with [$NiBr_2$-($PnBu$)$_2$], the products all exhibited colors and UV/Vis absorptions close to those for the precursor complexes or salts. The nonligated salts were thus solubilized upon encapulation. For [$RuCl_2(PPh_3)_3$], $FeBr_2$, [$NiCl_2(PPh_3)_2$], and [$NiBr_2(PPh_3)_2$], the encapsulation involved three in-core phosphines per complex (Table S3; by UV/Vis or ICP-AES), which suggests that the core-bound metals assume conformations similar to those of their precursor or original complexes. In contrast, **S3′** with [$NiBr_2(PnBu)_2$] (purple) turned green, in consistency with the change in ligand from the aliphatic to the aromatic phosphine (Figure 1 photos).

Based on the successful metal encapsulation, **S3** was employed as a catalyst carrier for a pentamethylcyclopentadienyl ruthenium complex [RuCp*Cl], known as an active catalyst for living radical polymerization. The tetrameric precursor [RuCp*Cl]$_4$[10] was mixed with **S3** in toluene at 80 °C for 12 h ([phosphine in **S3**]/[Ru] 2:1, assuming a double ligation to the metal center), to give RuCp*-Star **S4** without gellation and star–star coupling (Figure 1a). Near quantitative incorporation of [RuCp*Cl] was confirmed by UV/Vis (Figure 1b), ^{1}H and ^{31}P NMR spectroscopy, and ICP-AES (obd, 9000 ppm; calcd, 9350 ppm; over 96% incorporation), from which the ligation actually involves two phosphines of **2** per complex and almost all the ligands in the core (Figure 1c and d).

S4 was then applied to the polymerization of MMA with a chloride initiator [(MMA)$_2$Cl:**3**] in toluene at 80 °C (Figure 2, Table 1, Figure S5–S9). **S4** efficiently and homogeneously polymerized MMA to give poly(MMA) with narrow molecular weight distribution (MWD) and nearly quantitative end functionality (terminal olefin < 3 mol%; Table 1, entry 4; Figure S8). A sequential polymerization of MMA also proceeded upon in situ addition of fresh MMA into an as-obtained prepolymer solution with **S4** but without an additional catalyst feed (entry 5; Figure S9). The star polymer was robust enough to maintain the original shape and size during the polymerization (Figure S6). In contrast, the nonhydro-

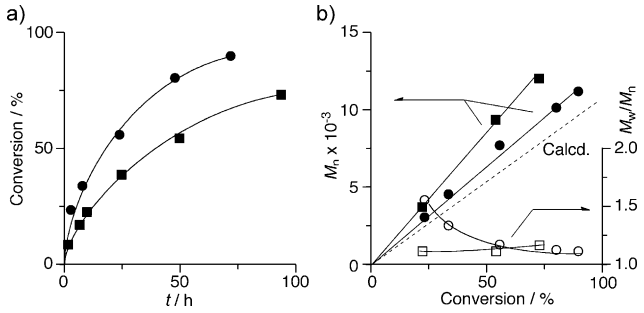

Figure 2. MMA polymerization catalyzed by **S4** (circles) and [RuCp*Cl-$(PPh_3)_2$] (squares; conditions: entries 4 and 6 in Table 1).

Table 1: MMA polymerization with various catalysts.[a]

Entry	Catalyst (in-core complex)	t [h]	Conversion [%][b]	M_n[c]	M_w/M_n[c]	Olefin [%][d]
1	**S1** ($RuCl_2$)	10	74	Gel	–	–
2	**S1** ($RuCl_2$)	10	46	Gel	–	–
3	**S3** (none)	24	0	–	–	–
4	**S4** ([RuCp*Cl])	72	90	11200	1.11	<3
5	**S4** ([RuCp*Cl])	144	197	20000	1.11	–
6	[RuCp*Cl$(PPh_3)_2$]	94	73	12000	1.16	≈ 30
7	[RuCp*Cl]$_4$	96	18	4800	2.27	–
8	RuCp*-Gel	72	89	20600	2.62	–
9	**S5** ($FeBr_2$)	144	81	8800	1.56	–
10	[$FeBr_2(PPh_3)_2$]	144	62	6700	1.20	–

[a] [MMA]/[ethyl α-chlorophenylacetate]/[Ru]/[nBu$_3$N] 2000:20 or 0:10:40 (entry 1 or 2); [MMA]/[**3**]/[core-PPh_3] 4000:40:8 (entry 3); [MMA]/[**3**]/[Ru] 4000:40:4.0 (entry 4, 6–8), 4000 + 4000:40:4.0 (entry 5), [MMA]/[$(MMA)_2$Br]/[Fe] 4000:40:4.0 (entry 9, 10) mM in toluene at 80 °C. [b] determined by GC [c] determined by SEC with DMF. [d] terminal olefins: determined by ^{1}H NMR spectroscopy.

genated version **S1** (with $RuCl_2$: Figure S7) resulted in insoluble products by gelation, both in the presence and in the absence of an externally added initiator (entries 1 and 2), hence indicating that the core-bound chlorine is still dormant and ready for radical dissociation. Thus, the halogen terminus removal by hydrogenation is essential for controlling polymerization with these in-core catalysts.

The catalytic activity and controllability of **S4** was superior to [RuCp*Cl$(PPh_3)_2$], a homogenous mimic of the **S4**-bound RuCp* (entry 6; Figure 2). The latter induced slower polymerization than **S4** to give products with a molecular weight ($M_n \approx 12000$) much higher than the calculated ($M_{n,calcd} \approx 7500$) and with a fairly large number of olefinic terminals (ca. 30%; entry 6). **S3** (empty core), [RuCp*Cl]$_4$, and RuCp*-Gel (RuCp* supported on a commercial microporous polystyrene gel) were invariably less effective (entries 3, 7, and 8; Figure S5). The tacticity of the products with **S4** and with [RuCp*Cl$(PPh_3)_2$] was similar: $mm/mr/rr = 4.8/37.0/58.2$ and 4.3/36.4/59.4, respectively (Figure S8).

Overall **S4** as catalyst has not only higher activity and better controlability but also higher stability, where the active RuCp*Cl complex is apparently well protected within the nanoscale ligating core network. $FeBr_2$-Star **S5**, similarly obtained from **S3** and $FeBr_2$, also gave a controlled product in higher yield (entry 9) than [$FeBr_2(PPh_3)_2$] (entry 10). This tendency is fully consistent with the higher activity and stability of **S5** in the radical addition of CCl_3Br to MMA than that of [$FeBr_2(PPh_3)_2$] (Figure S10).

Motivated by the high stability, we examined the tolerance of **S4** to functional groups (Table 2, Figure 3, S11). With its acid function often poisonous for metal catalysts, methacrylic acid (MAA) is normally unsuitable for metal-catalyzed living radical polymerization. In fact, [RuCp*Cl$(PPh_3)_2$] was not effective for MAA (entry 2). In contrast, **S4** efficiently copolymerized unprotected MAA (5 mol% in feed) with MMA, leading to narrow MWDs and high end functionality (entry 1) (^{1}H NMR spectroscopy: terminal olefin <3.7%; MAA content ca. 4.0%). This is the first example to show the direct and efficient copolymerization of MAA with metal catalysts.[15] The same star catalyst was also more effective for 2-hydroxyethyl methacrylate (HEMA) than [RuCp*Cl$(PPh_3)_2$] (entries 3 and 4; Figure S11). The high tolerance of functional groups most likely arises from the protection of catalytic metal species by the relatively rigid microgel network.

Table 2: Copolymerization of functional monomers (FMA) and MMA.

Entry[a]	FMA	Catalyst	Conversion,[b] MMA/FMA [%]	M_n[c]	M_w/M_n[c]
1	MAA	**S4**	75/72	8300	1.15
2	MAA	[RuCp*Cl$(PPh_3)_2$]	29/28	–	–
3	HEMA	**S4**	72/96	8000	1.13
4	HEMA	[RuCp*Cl$(PPh_3)_2$]	33/70	4400	1.17

[a] [MMA]/[FMA]/[**3**]/[Ru] 1900:100:20:4.0 mM in THF (entry 1,2); 1700:300:20:4.0 mM in toluene (entry 3,4) at 80 °C for 144 h. [b] Determined by ^{1}H NMR spectroscopy. [c] determined by SEC with DMF (entry 2: no detection due to the low molecular weight of the products).

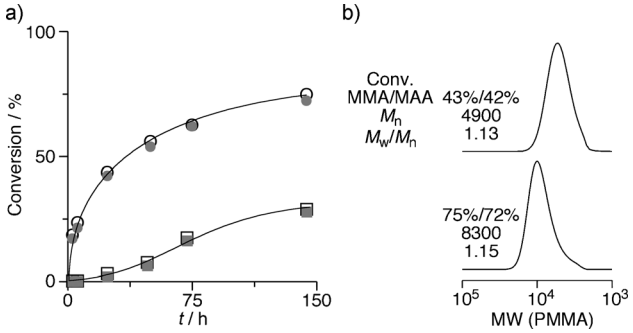

Figure 3. a) Copolymerization of MMA and MAA catalyzed by **S4** (black circles: MMA; gray circles: MAA) and [RuCp*Cl$(PPh_3)_2$] (black squares: MMA; gray squares: MAA) in THF at 80 °C (conditions: entries 1 and 2 in Table 2). b) SEC curves of the products obtained with **S4**.

S4 could also control styrene polymerization ($M_w/M_n \approx 1.1$; terminal chlorine approximately 100%; Figure 4 and S12). Interestingly, **S4** precipitated beyond 50% conversion because of the incompatibility of PMMA arms and the as-produced polystyrene. The supernatant contained polystyrene free of **S4**, as confirmed by SEC and UV/Vis, and ICP-AES (Ru residue: <56 ppm: over 95% removal by sponta-

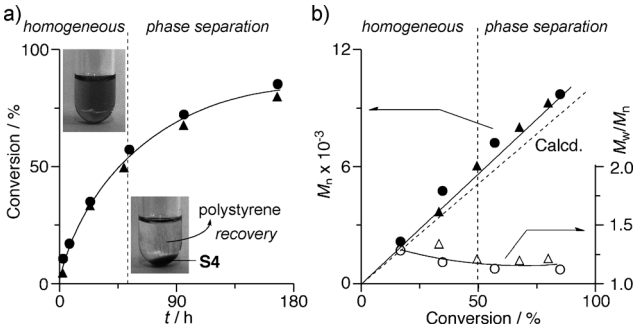

Figure 4. Catalyst recycling in **S4**-catalyzed polymerization of styrene (circles: first run; triangles: second run): [styrene]/[**3**]/[Ru] 4000:40:4.0 mM in toluene at 100 °C.

neous precipitation), and pure, white polystyrene was almost quantitatively recovered by simple evaporation. The precipitated catalyst was reusable for polymerization without any loss of activity and controlability (Figure 4): upon completion of the first polymerization, the supernatant solution (polystyrene and toluene) was removed by a syringe, and a fresh mixture of styrene and toluene was added to initiate the second run. In contrast, insoluble RuCp*-Gel gave uncontrolled products ($M_w/M_n > 2.0$; Figure S12).

In conclusion, we have successfully synthesized RuCp*-bearing star polymer catalysts **S4** by a one-pot tandem catalyst transformation coupled with ruthenium-catalyzed living radical polymerization, in situ hydrogenation, and the interchange of core-bound metals. Catalyst encapsulation into the core enabled the star polymers to work as unique reaction vessels with active, versatile, stable, and recyclable catalysts for living radical polymerization. Further space design of the microgel-core star polymer catalysts would open new possibilities for innovative catalysis.

Experimental Section

S4-catalyzed living radical polymerization was carried out by syringe technique under argon in baked glass tubes equipped with a three-way stopcock. $[RuCp^*Cl]_4$ (0.006 mmol, 6.52 mg), **S3** (0.048 mmol of PPh_3 ligand, 115 mg), and toluene (2.8 mL) were added to a Schlenk tube. The mixture was placed in an oil bath at 80 °C for 12 h to give **S4**. Into the in situ formed catalyst solution, *n*-octane (0.3 mL), MMA (24 mmol, 2.57 mL), and **3** (0.24 mmol, 0.33 mL of 720 mM toluene solution) were added at 25 °C under argon (total volume: 6.0 mL). Six aliquots (1.0 mL each) of the mother solution were distributed into baked glass tubes that were subsequently sealed and placed in an oil bath at 80 °C. After the predetermined period, the reaction was terminated by cooling to −78 °C. The conversion of MMA was determined by GC with *n*-octane as an internal standard. M_n and M_w/M_n were determined by SEC in $CHCl_3$ (PMMA standards).

Received: February 24, 2011
Revised: May 25, 2011
Published online: June 10, 2011

Keywords: living radical polymerization · ruthenium · star polymers · supported catalysts · tandem catalysis

[1] T. Uemura, N. Yanai, S. Kitagawa, *Chem. Soc. Rev.* **2009**, *38*, 1228–1236.
[2] B. Helms, J. M. J. Fréchet, *Adv. Synth. Catal.* **2006**, *348*, 1125–1148.
[3] D. E. Bergbreiter, J. Tian, C. Hongfa, *Chem. Rev.* **2009**, *109*, 530–582.
[4] a) H. Gao, K. Matyjaszewski, *Prog. Polym. Sci.* **2009**, *34*, 317–350; b) A. Blencowe, J. F. Tan, T. K. Goh, G. G. Qiao, *Polymer* **2009**, *50*, 5–32.
[5] a) T. Terashima, M. Kamigaito, K.-Y. Baek, T. Ando, M. Sawamoto, *J. Am. Chem. Soc.* **2003**, *125*, 5288–5289; b) T. Terashima, M. Ouchi, T. Ando, M. Sawamoto, M. Kamigaito, *Macromolecules* **2007**, *40*, 3581–3588; c) T. Terashima, M. Ouchi, T. Ando, M. Sawamoto, *J. Polym. Sci. Part A* **2010**, *48*, 373–379; d) T. Terashima, M. Ouchi, T. Ando, M. Sawamoto, *J. Polym. Sci. Part A* **2011**, *49*, 1061–1069.
[6] A. W. Bosman, R. Vestberg, A. Heumann, J. M. J. Fréchet, C. J. Hawker, *J. Am. Chem. Soc.* **2003**, *125*, 715–728.
[7] a) B. Helms, S. J. Guillaudeu, Y. Xie, M. McMurdo, C. J. Hawker, J. M. J. Fréchet, *Angew. Chem.* **2005**, *117*, 6542–6545; *Angew. Chem. Int. Ed.* **2005**, *44*, 6384–6387; b) Y. Chi, S. T. Scroggins, J. M. J. Fréchet, *J. Am. Chem. Soc.* **2008**, *130*, 6322–6323.
[8] S. Kanaoka, N. Yagi, Y. Fukuyama, S. Aoshima, H. Tsunoyama, T. Tsukuda, H. Sakurai, *J. Am. Chem. Soc.* **2007**, *129*, 12060–12061.
[9] M. Ouchi, T. Terashima, M. Sawamoto, *Chem. Rev.* **2009**, *109*, 4963–5050.
[10] a) M. Ouchi, M. Ito, S. Kamemoto, M. Sawamoto, *Chem. Asian J.* **2008**, *3*, 1358–1364; b) H. Yoda, K. Nakatani, T. Terashima, M. Ouchi, M. Sawamoto, *Macromolecules* **2010**, *43*, 5595–5601.
[11] S. Faucher, S. Zhu, *J. Polym. Sci. Part A* **2007**, *45*, 553–565.
[12] P. B. Zetterlund, Y. Kagawa, M. Okubo, *Chem. Rev.* **2008**, *108*, 3747–3794.
[13] T. Terashima, M. Ouchi, T. Ando, M. Sawamoto, *J. Am. Chem. Soc.* **2006**, *128*, 11014–11015.
[14] H. D. Maynard, R. H. Grubbs, *Tetrahedron Lett.* **1999**, *40*, 4137–4140.
[15] S. Ida, T. Terashima, M. Ouchi, M. Sawamoto, *J. Am. Chem. Soc.* **2009**, *131*, 10808–10809.

